Explosive percolation transitions in growing networks

S. M. Oh,[1] S.-W. Son,[2,*] and B. Kahng[1,†]
[1]*CCSS, CTP and Department of Physics and Astronomy, Seoul National University, Seoul 08826, Korea*
[2]*Department of Applied Physics, Hanyang University, Ansan 15588, Korea*
(Received 16 October 2015; revised manuscript received 4 January 2016; published 17 March 2016; corrected 22 March 2016)

Recent extensive studies of the explosive percolation (EP) model revealed that the EP transition is second order with an extremely small value of the critical exponent β associated with the order parameter. This result was obtained from static networks, in which the number of nodes in the system remains constant during the evolution of the network. However, explosive percolating behavior of the order parameter can be observed in social networks, which are often growing networks, where the number of nodes in the system increases as dynamics proceeds. However, extensive studies of the EP transition in such growing networks are still missing. Here we study the nature of the EP transition in growing networks by extending an existing growing network model to a general case in which m node candidates are picked up in the Achlioptas process. When $m = 2$, this model reduces to the existing model, which undergoes an infinite-order transition. We show that when $m \geqslant 3$, the transition becomes second order due to the suppression effect against the growth of large clusters. Using the rate-equation approach and performing numerical simulations, we also show that the exponent β decreases algebraically with increasing m, whereas it does exponentially in a corresponding static random network model. Finally, we find that the hyperscaling relations hold but in different forms.

DOI: 10.1103/PhysRevE.93.032316

I. INTRODUCTION

Percolation is a simple yet basic model for understanding the emergence of a giant component as links are occupied with a certain probability between each pair of nodes in a system [1,2]. This simple model has been applied to a variety of real-world phenomena such as the sol-gel transition [3–6], spreading of epidemic diseases [7–10], and the metal-insulator transition [11]. Conventionally, a percolation transition is second order [1,2]; however, interest in other types of percolation transitions such as first-order [12], infinite-order [13,14] or mixed-order [15] phase transitions has increased recently. This fashion has been triggered by the explosive percolation (EP) model [16] and an cascading failure model in interdependent networks [17,18].

An EP model was introduced aiming to generate a discontinuous percolation transition, in which two potential edges are chosen randomly, and then an actual connection is made by the edge that produces the smaller component. After extensive research was performed, it turned out that the EP model undergoes a second-order transition in the thermodynamic limit [19,20], even though it can be discontinuous when sufficient global information is imposed [21]. The critical exponent β of the order parameter for the original EP model is extremely small [19], implying that the order parameter increases drastically at a transition point. Moreover, properties of the EP transition are unconventional [22]. Such diverse features of the EP transitions were obtained mainly from static networks, in which the number of nodes is fixed from the beginning. However, real-world phenomena related to such a drastic increase of the order parameter can be observed in growing social networks [23]. Nevertheless, the EP transition on growing networks has not been investigated in detail yet [24,25]. Thus, this paper aims to investigate an EP transition on growing networks.

We recall a percolation model on growing networks, which exhibits an infinite-order phase transition [13]. In this model, at each time step, a node is added to the system, and then two distinct nodes are chosen randomly and connected with a certain probability p unless they are not connected yet. The model we consider here is a generalization of this existing model [13] by applying the so-called Achlioptas rule: Instead of choosing two nodes, we choose m distinct nodes. However, actual connection of an edge is made between the two nodes which are contained in the smallest two clusters among the m clusters to which the m selected nodes belong. When those two nodes are selected from the same cluster, they are connected but the size of that cluster does not change at all.

We investigate a percolation transition arising in the above model as the control parameter m is varied and show that the cluster size distribution changes drastically when the Achlioptas rule is applied. When the Achlioptas rule is absent ($m = 2$), the cluster size distribution follows a power law not only at the transition point $p = p_c$ but also below p_c; however, when the Achlioptas rule is present ($m \geqslant 3$), it exhibits the critical behavior only at p_c but a subcritical behavior for $p < p_c$. The Achlioptas rule yields the suppression effect against the growth of large clusters, leading to the change of the tail part of the cluster size distribution from a power law to an exponentially decaying form for $p < p_c$. Thus, the transition type changes from infinite order to second order. We also show that the critical exponent β decreases with m algebraically on the growing network model, whereas it does exponentially on static network models [26,27]. This property reflects that the suppression effect can be weaker on growing network models than that on static network models. Moreover, we obtain the critical exponents and their m dependency for the growing network model and compare the results with those for a corresponding static network model we introduce later.

The paper is organized as follows: The model we study is introduced in Sec. II, and the rate equation of the cluster size

*sonswoo@hanyang.ac.kr
†bkahng@snu.ac.kr

distribution for the growing and the static network models are derived in Sec. III. Finite-size scaling analysis is performed for the growing and the static network models with $m = 3$ in Sec. IV. The obtained critical exponents are compared with those obtained from the rate-equation approach. In Sec. V, the cluster size distribution for the original growing percolation model, which exhibits an infinite-order phase transition, is presented to compare it with those obtained from the explosive percolation in the growing network model exhibiting a second-order transition.

II. TWO TYPES OF NETWORK MODELS: GROWING AND STATIC

In this paper, we introduce two types of network models: growing and static. In a growing network model, the number of nodes increases one by one at each time step, whereas in a static network model, the number of nodes is fixed from the beginning. Edges are added one by one at each time step in both models according the following rules:

(i) The growing network model begins with an isolated node, and at each time step, a node is added in the system. Thus, the number of nodes $N(t)$ at time t becomes $N(t) = t + 1$. Next, m candidate nodes are selected randomly. When $N(t)$ is less than m, all nodes are regarded as candidates. When $N(t) \geqslant m$, m nodes are selected randomly, and their m clusters are identified. Some of those clusters can be identical when more than one selected nodes are contained in the same cluster. The two selected nodes belonging to the smallest two clusters among those m clusters are connected with probability p unless they are already connected. When $m = 2$, this growing network model reduces to an existing growing network model proposed by Callaway *et al.* [13].

(ii) The static network model contains N isolated nodes from the beginning and they remain fixed. At each time step, m candidate nodes are selected uniformly at random, and the two nodes among them, which belong to the smallest two clusters, are connected with probability one. When $m = 2$, this static network model reduces to the Erdős-Rényi (ER) random network model [28].

III. RATE EQUATION APPROACH FOR THE CLUSTER SIZE DISTRIBUTION

A. The growing network model with $m = 3$

Let $n_s(p,t)$ be the number of clusters of size s divided by $N(t)$ at time step t, where p denotes the probability that a link is connected between the two selected nodes. The rate equation of $n_s(p,t)$ is given by

$$\frac{d(N(t)n_s)}{dt} = p\Bigg[\sum_{i+j=s;i<j} 3in_i(jn_j)^2 + \sum_{i+j=s;i<j} 6in_i jn_j c_{j+1} + \left(\frac{s}{2}n_{\frac{s}{2}}\right)^3 + 3\left(\frac{s}{2}n_{\frac{s}{2}}\right)^2 (c_{\frac{s}{2}+1}) - 2(sn_s)^3 - 6(sn_s)^2 c_{s+1} - 3(sn_s)^2(1-c_s) - 3sn_s(c_{s+1})^2 - 6sn_s(1-c_s)c_{s+1}\Bigg] + \delta_{1s}, \quad (1)$$

where n_i denotes $n_i(p,t)$ and $c_s(p,t) = 1 - \sum_{i<s} in_i(p,t)$.

The first term, $3in_i(jn_j)^2$, of the right-hand side of Eq. (1) comes from the merging of two clusters of size i and j under the constraint $i < j$, which produces a cluster of size $s = i + j$. One node is selected from a cluster of size i and the other two nodes are selected from either (i) one cluster of size j or (ii) two distinct clusters of size j. However, the probability to occur the case (i) is $j\frac{N_i}{N}\frac{j}{N}$, which is much smaller than $(j\frac{N_j}{N})^2$ for the case (ii), and thus the first case was ignored. The factor 3 comes from the combinatorics of the three possible clusters. For simplicity, this process is denoted as $(i, j > i, j > i)_{i+j=s}$. The second term comes from the process $(i, j > i, k > j)_{i+j=s}$. This means that the three nodes are chosen from the clusters of different sizes i, j, and k under the constraint $i < j < k$, and the two smallest clusters of sizes i and j are merged. Since the size k can be arbitrary as long as $k > j$, we used $c_{j+1} \equiv \sum_{k>j} kn_k$ instead of kn_k. The factor 6 again comes from the combinatorics. The third term comes from the process $(\frac{s}{2}, \frac{s}{2}, \frac{s}{2})$, which represents that three nodes are chosen from three distinct clusters of size $s/2$. Similarly, the fourth term comes from the process $(\frac{s}{2}, \frac{s}{2}, k > \frac{s}{2})$, which means that two nodes are chosen from two distinct clusters of size $s/2$ and the other node are chosen from a cluster of size k larger than $s/2$. Note that if two nodes are chosen from the same cluster of size $s/2$, then there is no cluster merging and the probability of this case occurring becomes $\frac{s}{2}\frac{N_{s/2}}{N}\frac{s/2}{N}$, which is smaller than $(\frac{s}{2}n_{\frac{s}{2}})^2$. Thus, this case was ignored. The factor 3 again comes from the combinatorics. The third and fourth terms appear only when s is even. Up to this point all terms are for the creation of s-size clusters.

The terms from the fifth to the ninth are for the annihilation of s-size clusters. The fifth and the sixth terms come from the processes (s,s,s) and $(s,s,k > s)$, respectively. These two terms correspond to the third and the fourth terms presented above. But the prefactors are 2 times bigger because two clusters of size s merge and annihilate simultaneously. The seventh term comes from the process $(s,s,k < s)$, which represents that two nodes are chosen from two distinct clusters of size s and the other node is chosen from a cluster of size k smaller than s. Again, we note that we ignore the case where two or more nodes are selected from the same one cluster, because that case occurs with smaller probability than that of two or more nodes being selected from distinct clusters in the limit $N(t) \to \infty$. The factor 3 again comes from the combinatorics. The eighth term comes from the process $(s,i > s,i > s)$, which represents the case that one node is chosen from a cluster of size s and the other two nodes are chosen from the clusters of size i larger than s. The factor 3 again comes from the combinatorics. The ninth term comes from the process $(s,i < s, j > s)$, which means that three nodes are chosen from three different-size clusters: clusters of size s, of smaller than s, and of bigger than s, respectively. The factor 6 comes from the combinatorics. Overall, factor p is the probability that the two nodes determined are connected. The last term δ_{1s} arises when a node is added to the system at each time step.

The rate equation was set up under the following approximations, which are valid in the long-time limit, $N(t) \to \infty$. To be specific, let us suppose that the process generating the first term of the right-hand side of Eq. (1) is $3in_i(jn_j)^2$. The

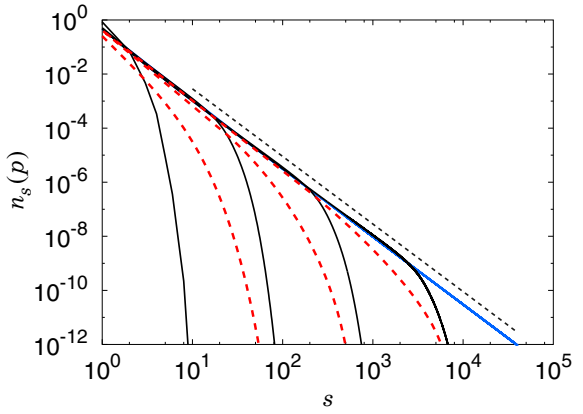

FIG. 1. The growing network model with $m = 3$: Plot of $n_s(p)$ versus s at $p = p_c$ (blue solid line), $p > p_c$ (red dashed curves), and $p < p_c$ (black solid curves) based on numerical values obtained from the rate equation. The transition point p_c and the exponent τ are estimated as $p_c = 0.413842(1)$ and 2.5, respectively. The black dotted line is a guide line with slope -2.5.

probability of picking up two nodes from two distinct clusters of equal size j is given as $\frac{jN_j}{N}\frac{j(N_j-1)}{N}$. We approximate this probability as $(jn_j)^2$ under the assumption that N_j is larger than 1. We also exclude the case in the rate equation that more than one node is selected from the same cluster. For instance, when two nodes are selected from single cluster of size j, the probability becomes $\frac{jN_j}{N}\frac{j}{N}$, which is regarded negligible compared with $\frac{jN_j}{N}\frac{jN_j}{N}$. We believe that this approximation is valid in the limit $N(t) \to \infty$.

Based on this rate equation, we calculate $n_s(p)$ in the steady state up to a certain size s^*, for instance, $s^* = 10^6$. Note that $n_s(p)$ decays in a power-law way as $n_s(p_c) \sim s^{-\tau}$ at a transition point p_c and exhibits crossover behavior $n_s(p) \sim s^{-\tau}\exp(-s/s_c)$ for $p \neq p_c$ with $s_c \sim |p - p_c|^{-1/\sigma}$ [1,2]. When $p > p_c$, an infinite cluster exists separately from finite clusters. The percolation threshold is estimated as $p_c = 0.413842(1)$ using the criterion that $n_s(p_c)$ follows power law at p_c as shown in Fig. 1. Moreover, the exponent τ is determined as $\tau \approx 2.5$. We also check the crossover behaviors for $p < p_c$ and $p > p_c$ in Fig. 1. The exponent σ is obtained by scaling the plots of $n_s(p)s^\tau$ versus $s|p - p_c|^{1/\sigma}$ for different p values. It can be shown that the data are well collapsed onto a single curve with $\sigma \approx 0.72$ (Fig. 2).

Next, the order parameter is obtained using the relation, $G(p) \approx 1 - \sum_{s=1}^{s^*} sn_s(p)$ [1,2], where s^* is a characteristic size which distinguishes an infinite cluster from finite clusters. We take several cluster sizes for s^* to check whether $G(p)$ depends on the chosen candidates of s^*. The obtained order parameter follows a power-law form, $G(p) \sim (p - p_c)^\beta$, where $\beta = 0.694(2)$. The inset of Fig. 3 is a double logarithmic plot of the order parameter as a function of $(p - p_c)$, which exhibits power-law behavior as expected. The obtained value of β satisfies the scaling relation $\beta = (\tau - 2)/\sigma$ [1,2].

The mean cluster size $\langle s\rangle$ is obtained from the cluster size distribution as $\langle s\rangle = \sum_{s=1}^{s^*} s^2 n_s(p)$, which diverges as $\langle s\rangle \sim (p - p_c)^{-\gamma_p}$ for $p > p_c$ and $(p_c - p)^{-\gamma'_p}$ for $p < p_c$. We also determine $\gamma_p = \gamma'_p = 0.696 \pm 0.003$. The numerical

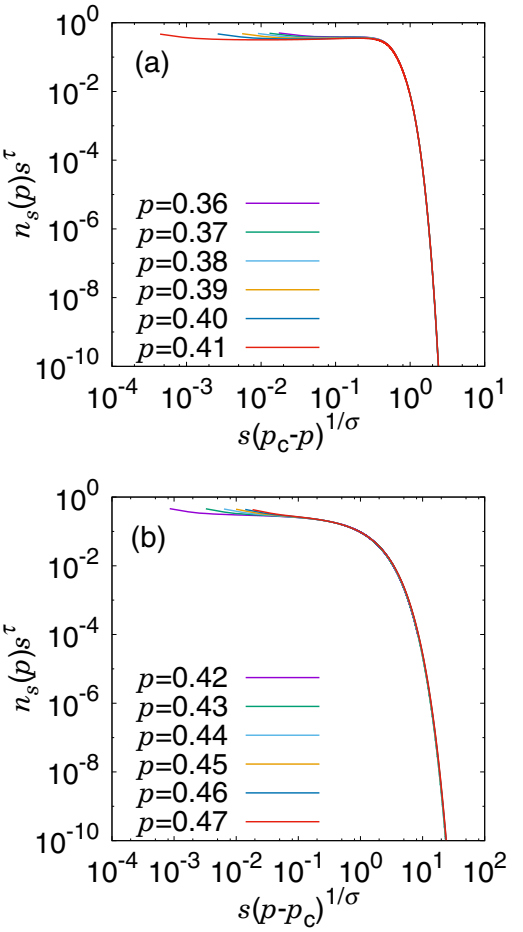

FIG. 2. The growing network model with $m = 3$: Scaling plot of $n_s(p)s^\tau$ versus $s|p - p_c|^{1/\sigma}$ for different values of p in the region (a) $p < p_c$ and (b) $p > p_c$. Data for different p values are well collapsed onto a single curve by choosing $\sigma = 0.720(2)$ and $\tau = 2.500(1)$.

values obtained from the rate equation are shown in Fig. 4. In the insets, $\langle s\rangle$ is plotted in double logarithmic axes as a function of $p - p_c$ for $p > p_c$ and $p_c - p$ for $p < p_c$. The exponent γ_p satisfies the well-known scaling relation $\gamma_p = (3 - \tau)/\sigma$ [1,2].

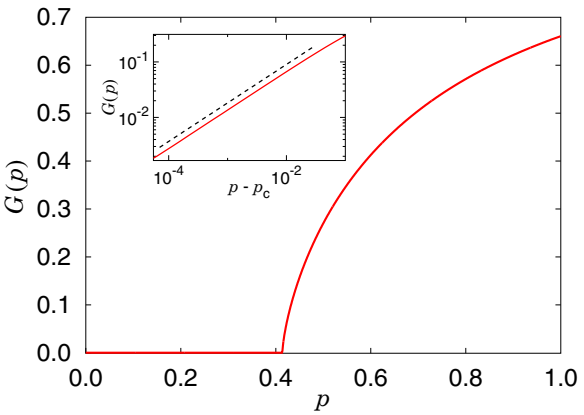

FIG. 3. The growing network model with $m = 3$: Plot of $G(p)$ versus p. Data points are obtained from the rate equation. Inset: Dashed line is a guideline with slope 0.694(2).

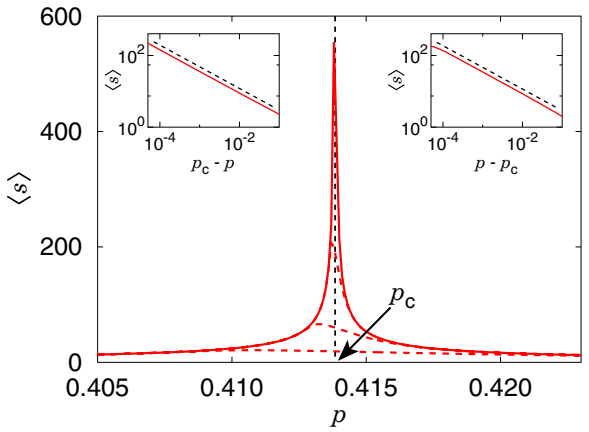

FIG. 4. The growing network model with $m = 3$: Plot of the mean cluster size $\langle s \rangle$ as a function of p. Data points are obtained from the rate equation. To take into account of finite-size effect, we truncate cluster size at given sizes $s^* = 10^3, 10^4, 10^5$ (dashed curves from below), and 10^6 (solid curve). Insets: Plots of $\langle s \rangle$ versus $|p - p_c|$ for $p < p_c$ (left) and $p > p_c$ (right). Dashed lines are guidelines with slope $-0.696(3)$.

B. The growing network model with general m

We extend the rate equation Eq. (1) to the one for arbitrary m as follows:

$$\frac{d(N(t)n_s)}{dt} = p\Bigg[\sum_{r=1}^{m-1} m\binom{m-1}{r-1} \sum_{i+j=s;i<j} i n_i (j n_j)^{m-r} (c_{j+1})^{r-1} + \sum_{r=1}^{m-1} \binom{m}{r-1}\left(\frac{s}{2} n_{\frac{s}{2}}\right)^{m-(r-1)} (c_{\frac{s}{2}+1})^{r-1} - 2\sum_{r=2}^{m}\binom{m}{r}(s n_s)^r (c_{s+1})^{m-r} - m(s n_s)(c_{s+1})^{m-1} - \sum_{r=1}^{m-1} m\binom{m-1}{r}(1-c_s)(s n_s)^r (c_{s+1})^{m-1-r}\Bigg] + \delta_{1s}. \quad (2)$$

Again, the second term on the right-hand side is valid only when s is even. Repeating the steps taken for the case $m = 3$, we obtain the critical exponents $\tau, \sigma, \beta, \gamma_p$, and the percolation threshold p_c up to $m = 10$, which are listed in Table I.

Following the conventional formalism for the second-order percolation transition, we examine m dependencies of the critical exponents. We find that the transition point p_c and the critical exponent β seem to behave as $1 - p_c \approx 1.81/m$ and $\beta \approx 1/(m - 1.56)$, as shown in Fig. 5. However, rigorous derivation of those formulas is still needed. Next, we estimate the exponents τ and σ for $m = 4, \ldots, 10$ by following similar steps used for $m = 3$. We find that the estimated values seem to fit to the formulas $\tau = 2 + 1/(m - 1)$ and $1/\sigma = (m - 1)\beta$ as shown in Fig. 6. Furthermore, we find that γ_p seems to behave as $(m - 2)\beta$.

TABLE I. The growing network model: Numerical estimates of p_c, τ, σ, β, and γ_p for $m = 3, \ldots, 10$. $\tilde{\tau}$ and $\tilde{\beta}$ were obtained from the empirical formulas $\tilde{\tau} = 2 + 1/(m - 1)$ and $\tilde{\beta} = 1/(m - 1.56)$, respectively.

m	p_c	$\tilde{\tau}$	τ	σ	$\tilde{\beta}$	β	γ_p
3	0.413842(1)	$\frac{5}{2}$	2.500(1)	0.720(2)	0.694	0.694(2)	0.696(3)
4	0.555873(1)	$\frac{7}{3}$	2.333(1)	0.812(2)	0.410	0.410(2)	0.813(3)
5	0.642748(1)	$\frac{9}{4}$	2.250(1)	0.858(2)	0.291	0.291(1)	0.874(6)
6	0.701282(1)	$\frac{11}{5}$	2.200(1)	0.885(2)	0.225	0.226(1)	0.904(2)
7	0.743370(1)	$\frac{13}{6}$	2.167(1)	0.905(2)	0.184	0.184(1)	0.922(2)
8	0.775078(1)	$\frac{15}{7}$	2.143(1)	0.918(2)	0.155	0.156(1)	0.934(2)
9	0.799820(1)	$\frac{17}{8}$	2.125(1)	0.928(2)	0.134	0.135(1)	0.944(3)
10	0.819663(1)	$\frac{19}{9}$	2.111(1)	0.936(2)	0.119	0.119(1)	0.950(3)

C. The static network model with $m = 3$

We consider the evolution of the static network model under the rule described in Sec. II. In this case, the number of nodes is fixed all the way under the evolution of the network. The

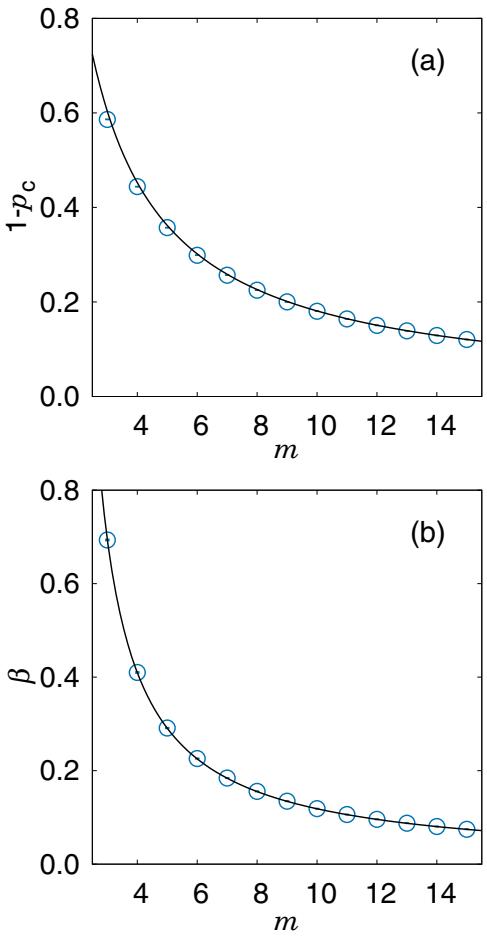

FIG. 5. The growing network model: (a) Plot of $1 - p_c$ versus m. Data points obtained from the rate equation seem to fit to the formula $1 - p_c = 1.81/m$. (b) Plot of β versus m. Data points obtained from the rate equation seem to fit to the formula $\beta = 1/(m - 1.56)$.

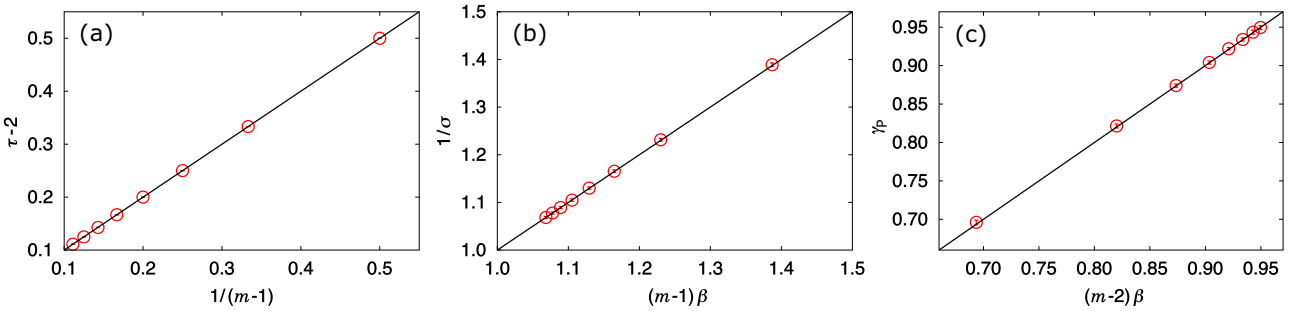

FIG. 6. The growing network model: shown are the testings whether the empirical formulas for the exponents (a) $\tau - 2 = 1/(m-1)$, (b) $1/\sigma = (m-1)\beta$, and (c) $\gamma_p = (m-2)\beta$ are correct. Data points are obtained from the rate equation.

rate equation is written as

$$N\frac{dn_s}{dt} = \sum_{i+j=s;i<j} 3in_i(jn_j)^2 + \sum_{i+j=s;i<j} 6in_i jn_j c_{j+1} + \left(\frac{s}{2}n_{\frac{s}{2}}\right)^3 + 3\left(\frac{s}{2}n_{\frac{s}{2}}\right)^2 (s_{\frac{s}{2}+1}) - 2(sn_s)^3 - 6(sn_s)^2 c_{s+1} - 3(sn_s)^2(1-c_s) - 3sn_s(c_{s+1})^2 - 6sn_s(1-c_s)c_{s+1}, \quad (3)$$

where n_i denotes $n_i(t)$ and $c_s(t) = 1 - \sum_{i<s} in_i(t)$. The terms with $n_{\frac{s}{2}}$ are valid only when s is even. In contrast to the case of the growing network model, there is no steady state in the size distribution, and n_s depends on t. Accordingly, it takes longer time to evaluate $n_s(t)$ explicitly compared with that for the growing network model. We obtain $n_s(t)$ up to a certain cluster size $s^* = 5 \times 10^5$.

We determine the percolation threshold t_c as shown in Fig. 7 based on the criterion that the cluster size distribution follows power law at t_c. It is obtained that $t_c = 0.849130(1)$ and $n_s(t_c) \sim s^{-\tau}$ with $\tau \approx 2.105$. For $t < t_c$ and $t > t_c$, the cluster size distribution exhibits a crossover behavior as $n_s(t) \sim s^{-\tau} \exp(-s|t-t_c|^{1/\sigma})$. Using the data-collapse method, we obtain $\sigma \approx 0.79$ as shown in Fig. 8.

Next, we consider behavior of the order parameter $G(t)$ at time step t. The order parameter is calculated using the relation $G(t) = 1 - \sum_{s=1}^{s^*} sn_s(t)$. We expect that $G(t) \sim (t-t_c)^\beta$ and obtain $\beta = 0.133(1)$ in Fig. 9. We also obtain the mean cluster size defined as $\langle s \rangle = \sum_{s=1}^{s^*} s^2 n_s(t)$. Following the convention, it behaves as $\langle s \rangle \sim |t-t_c|^{-\gamma_p}$. We estimate that $\gamma_p = 1.131(6)$ in Fig. 10. The obtained exponent values $\beta \approx 0.133$ and $\gamma_p \approx 1.133$ satisfy the scaling relation $\beta = (\tau-2)/\sigma$ and $\gamma_p = (3-\tau)/\sigma$, respectively.

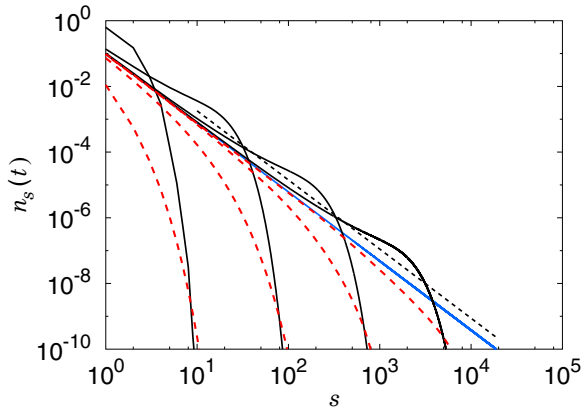

FIG. 7. The static network model with $m = 3$: Plot of $n_s(t)$ versus s at $t = t_c$ (blue solid line), for $t > t_c$ (red dashed curves), and for $t < t_c$ (black solid curves) based on numerical values obtained from the rate equation. The transition point t_c is determined as $t_c = 0.849130(1)$ and the exponent τ is estimated as $\tau = 2.105(5)$. The black dotted line is a guideline with the slope -2.105.

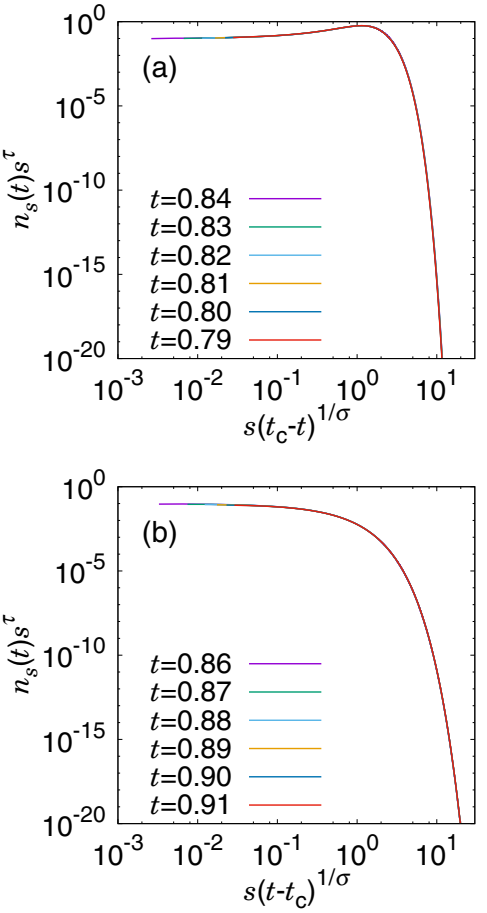

FIG. 8. The static network model with $m = 3$: Scaling plot of $n_s(t)s^\tau$ versus $s|t-t_c|^{1/\sigma}$ (a) for $t < t_c$ and (b) for $t > t_c$. Data points are well collapsed by taking $\tau = 2.105(5)$ and $\sigma = 0.790(1)$.

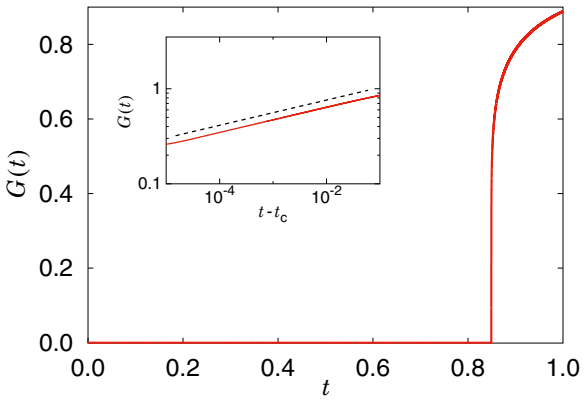

FIG. 9. The static network model with $m = 3$: Plot of the order parameter $G(t)$ as a function of t. Inset: The dotted line is a guideline with the slope 0.133(1).

D. The static network model with general m

We extend the rate equation for $m = 3$ to the one for arbitrary m as follows:

$$N\frac{dn_s}{dt} = \sum_{r=1}^{m-1} m\binom{m-1}{r-1} \sum_{i+j=s;i<j} in_i(jn_j)^{m-r}(c_{j+1})^{r-1} + \sum_{r=1}^{m-1}\binom{m}{r-1}\left(\frac{s}{2}n_{\frac{s}{2}}\right)^{m-(r-1)}(c_{\frac{s}{2}+1})^{r-1} - 2\sum_{r=2}^{m}\binom{m}{r}(sn_s)^r(c_{s+1})^{m-r} - m(sn_s)(c_{s+1})^{m-1} - \sum_{r=1}^{m-1} m\binom{m-1}{r}(1-c_s)(sn_s)^r(c_{s+1})^{m-1-r}, \quad (4)$$

where the term for $n_{\frac{s}{2}}$ is valid only when s is even.

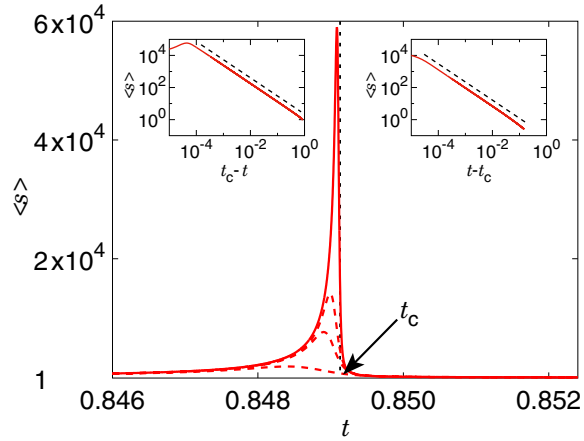

FIG. 10. The static network model with $m = 3$: Plot of $\langle s\rangle$ as a function of t. To take into account the finite-size effect, we truncate cluster size at given sizes $N_c = 10^4, 5\times10^4, 10^5$ (dashed curves from below), and 5×10^5 (solid curve). Inset: Plot of the mean cluster size as a function of t for $t > t_c$ (right) and for $t < t_c$ (left). Both dashed lines are guidelines with slope $-1.131(6)$.

TABLE II. The static network model: Numerical estimates of t_c, τ, σ, and β and γ_p for $m = 2,\ldots,5$. $\tilde\tau$ and $\tilde\beta$ were obtained from the empirical formulas $\tilde\tau = 2 + \beta/[1 + (m-1)\beta]$ and $\tilde\beta \approx 0.465\exp(-0.70m)$, respectively.

m	t_c	$\tilde\tau$	τ	σ	$\tilde\beta$	β	γ_p
2	0.5	2.5	2.5	0.5	0.115	1	1
3	0.849130(1)	2.105	2.105(1)	0.790(1)	0.057	0.133(1)	1.131(6)
4	0.939678(1)	2.037	2.037(1)	0.890(1)	0.028	0.042(1)	1.082(6)
5	0.972672(1)	2.016	2.015(2)	0.940(1)	0.014	0.017(1)	1.050(4)

Taking similar steps used for $m = 3$, we determine the transition point and the critical exponent β for general m up to $m = 15$. It is likely that these values behave asymptotically as $1 - t_c \approx \exp(-0.59m)$ and $\beta \approx \exp(-0.70m)$, respectively. This conjecture was also alluded in Refs. [26,27]. A numerical test is shown in Fig. 11.

Furthermore, we determine the exponent values τ and σ for $m = 4$ and $m = 5$. The obtained values are listed in Table II. Notice that the values approximate to the formulas $\tau = 2 + \beta/[1 + (m-1)\beta]$ and $1/\sigma = 1 + (m-1)\beta$ as shown in Fig. 12.

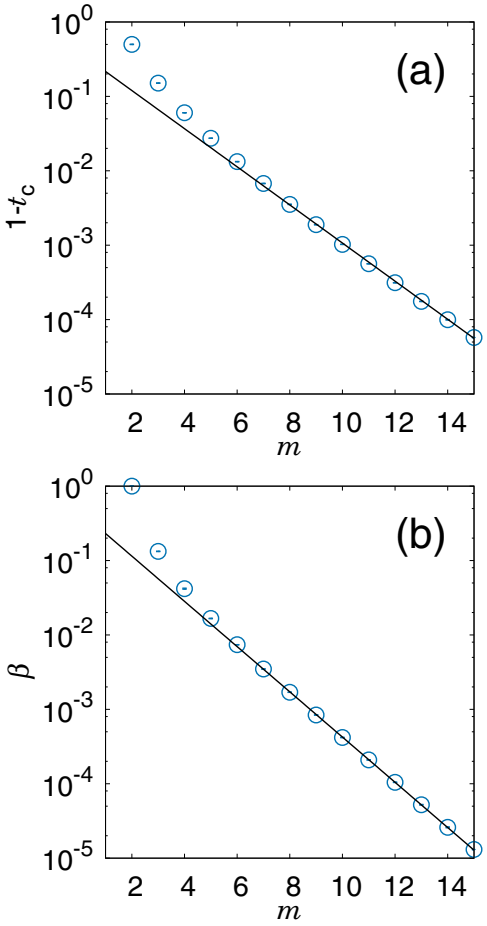

FIG. 11. The static network model: (a) Plot of estimated values of $1 - t_c$ versus m on a semilogarithmic scale. (b) Plot of estimated values of β versus m on a semilogarithmic scale. Data points likely lie on a straight line asymptotically. The error bar of each data point is smaller than the respective symbol size.

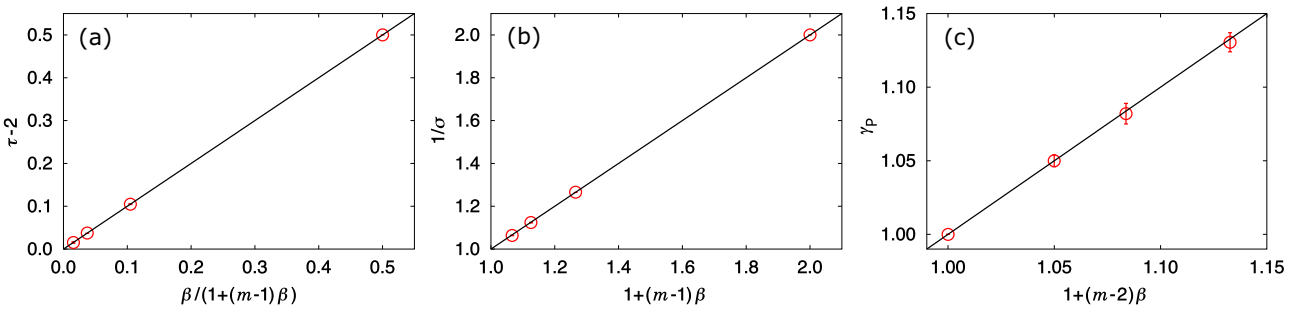

FIG. 12. The static network model: Shown are the testings of whether the empirical formulas for (a) τ, (b) σ, and (c) γ_p are fit to numerical data points obtained from the rate equation.

This conclusion is based on the previous analytic solution for a slightly different static network model in [26,27]. Since the value of m in our model corresponds to $2m$ in the model [26,27], the analytic solution in Refs. [26,27] is valid to our model but with replacing $2m$ with m. This allows us to obtain $\gamma_p = 1 + (m-2)\beta$.

IV. FINITE-SIZE SCALING ANALYSIS

A. Hyperscaling relations in explosive percolation

In EP, the susceptibility was defined in unconventional way [27] using the correlation function $C(i,j)$ as follows:

$$\chi = \frac{1}{N}\sum_{i,j=1}^{N} C(i,j), \tag{5}$$

where $C(i,j)$ is the correlation function, defined as $C(i,j) = 1$ if nodes i and j belong to the same cluster and $C(i,j) = 0$ otherwise. The susceptibility diverges at the critical point as $\chi \sim |p - p_c|^{-\gamma}$ for the growing network model and $\chi \sim |t - t_c|^{-\gamma}$ for the static network model. It was shown that in the EP problem, the hyperscaling relations are given as (i) $d_f = 1/(\sigma\nu)$, (ii) $d_f = d - \beta/\nu$, and (iii) $d - 2 + \eta = 2\beta^*/\nu$. Here β^* is the exponent of the so-called observable order parameter, which is modified from the exponent β to take into account of the effect of choosing m candidates.

In our model, according to the dynamic rule, the probability that the two nodes belong to the giant cluster is $x_{\rm pc}^2$, where $x_{\rm pc}$ denotes the probability to select a node in the giant cluster (following the notation in Ref. [27]). To choose the two nodes from the giant cluster, the other $m-2$ candidate nodes have no choice but to belong to the same giant cluster. Thus, the probability to choose m nodes from the giant cluster is given as G^m. Thus, $x_{\rm pc} = G^{m/2}$, leading to $\beta^* = (m/2)\beta$. On the other hand, in Eq. (5), if we take integral range as $[0,\xi]$, then we can obtain the relation $2 - \eta = \gamma/\nu$. Thus, the hyperscaling relation (iii) can be expressed in a different form (iv) $2\beta^* + \gamma = d\nu$. In the following subsections, we will check if the hyperscaling relations (iii) and (iv) hold in the growing and the static network models.

B. Simulation results for the growing network model with $m = 3$

To determine the exponents τ and σ of the cluster size distribution, we perform numerical simulations for the growing network model with different system sizes $N/10^4 = 2^3 - 2^{10}$. The ensemble average is taken over 10^4 runs.

We first examine the cluster size distribution for several values of p around the transition point p_c in Fig. 13. The cluster size distribution follows a power law at p_c and exhibits the crossover behavior of $n_s(p) \sim s^{-\tau}\exp(-s|p-p_c|^{1/\sigma})$. We determine $p_c = 0.4138(2)$ using the criteria that at p_c, $n_s(p_c)$ decays in a power-law way and the size of the giant cluster per node, $G_N(p_c)$, follows a power law, $G_N(p_c) \sim N^{-\beta/\bar{\nu}}$. Using

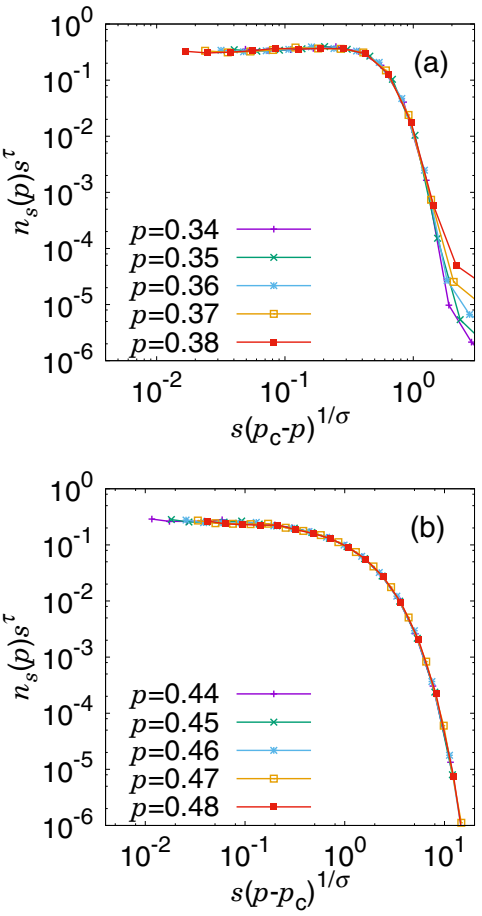

FIG. 13. The growing network model with $m = 3$: Scaling plot of $n_s(p)s^\tau$ versus $s|p - p_c|^{1/\sigma}$. Data points are obtained from Monte Carlo simulations. Data collapse is established onto a single curve by choosing $\tau = 2.5$ and $\sigma = 0.72$ for (a) $p < p_c$ and for (b) $p > p_c$.

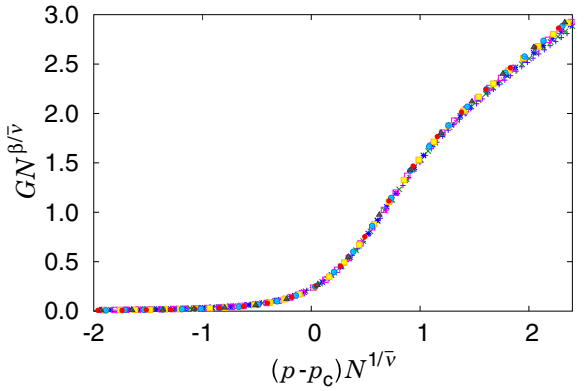

FIG. 14. The growing network model with $m = 3$: Scaling plot of $GN^{\beta/\bar{\nu}}$ versus $(p - p_c)N^{1/\bar{\nu}}$ for the system sizes $N/10^4 = 2^3 - 2^{10}$. Data points obtained from numerical simulations are well collapsed onto a single curve with $1/\bar{\nu} = 0.35(3)$ and $\beta/\bar{\nu} = 0.24(3)$.

the data-collapse method, we determine the exponent values of τ and σ to be $\tau \approx 2.5$ and $\sigma \approx 0.72$, respectively, which are in good agreement with the values obtained by the rate-equation approach.

By direct measuring the exponent β of $G_N(p_c)$ and using the finite-size scaling formula $G_N(p) = N^{-\beta/\bar{\nu}} f[(p - p_c)N^{1/\bar{\nu}}]$, we determine the ratios $\beta/\bar{\nu} = 0.24(3)$ and $1/\bar{\nu} \approx 0.35(3)$, as shown in Fig 14. We determine $\beta \approx 0.69$. These values are consistent with those obtained from the rate equation.

The mean cluster size is also examined by plotting it in a scaling form, i.e., $\langle s \rangle N^{-\gamma_p/\bar{\nu}}$ versus $(p - p_c)N^{1/\bar{\nu}}$ with $\gamma_p = 0.70 \pm 0.03$ and $1/\bar{\nu} = 0.35$ in Fig. 15 for different system sizes $N/10^4 = 2^6 - 2^{10}$. Ensemble average is taken over 10^4 runs. Data are well collapsed.

Next, to check the hyperscaling relations, we use the obtained values of $\beta/\bar{\nu}$ and $1/\bar{\nu}$ and calculate $\beta = 0.70 \pm 0.15$ ($\beta^* = 1.05 \pm 0.22$ for $m = 3$) and $\bar{\nu} = 2.88 \pm 0.25$. In the mean-field limit, the hyperscaling relation becomes $d_u - 2 = 4\beta^*$, where d_u denotes the upper critical dimension, $\eta = 0$ and $\nu = 1/2$. Using the value of β^*, we obtain $d_u = 6.19 \pm 0.87$ and the correlation volume exponent $\bar{\nu}' \equiv d_u \nu = 3.10 \pm 0.44$, which is roughly consistent with the directly measured value $\bar{\nu} = 2.88 \pm 0.25$ within the error bars. Thus, the hyperscaling relation $d_u - 2 + \eta = 2\beta^*/\nu$ holds. Moreover, using $\beta^* = 1.05 \pm 0.22$ and $\gamma = 1$, we obtain $2\beta^* + \gamma = 3.10 \pm 0.44$. This value is consistent with $\bar{\nu}'$ and the measured value within the error bar. Thus, the hyperscaling relation $2\beta^* + \gamma = \bar{\nu}$ also holds.

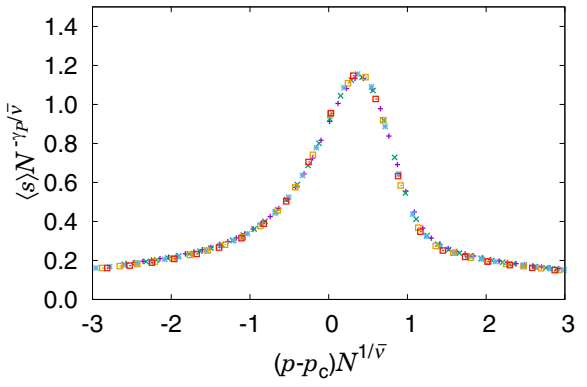

FIG. 15. The growing network model with $m = 3$: Scaling plot of $\langle s \rangle N^{-\gamma_p/\bar{\nu}}$ versus $(p - p_c)N^{1/\bar{\nu}}$ for different system sizes $N/10^4 = 2^6 - 2^{10}$. Data obtained from numerical simulations are well collapsed onto a single curve with $\gamma_p = 0.696$ and $1/\bar{\nu} = 0.35$.

C. Simulation results for the static network model with $m = 3$

To determine the exponents τ and σ for the cluster size distribution, we perform Monte Carlo simulations for the static network model of different system sizes $N/10^4 = 2^7 - 2^{10}$. The ensemble average was taken over 10^5 for each data point. The cluster size distributions $n_s(t)$ for different times are plotted in a scaling form, i.e., $n_s(t) \sim s^{-\tau} \exp(-s|t - t_c|^{1/\sigma})$, as shown in Fig. 16. Using the previously obtained values $t_c = 0.84913(1)$ and $\tau \approx 2.1$, we find that the data for different t are well collapsed onto a single curve with $\sigma = 0.79$.

Next, we consider the order parameter $G_N(t)$ as a function of time t for different system sizes $N/10^4 = 2^7 - 2^{10}$. The critical point t_c and the critical exponent β are determined using the scaling ansatz $G_N(t) = N^{-\beta/\bar{\nu}} f[(t - t_c)N^{1/\bar{\nu}}]$. Based on the criterion that $G_N(t) \sim N^{-\beta/\bar{\nu}}$ at $t = t_c$, we determine $t_c = 0.84913(1)$ and $\beta/\bar{\nu} \approx 0.06(1)$ in Fig. 17. Moreover,

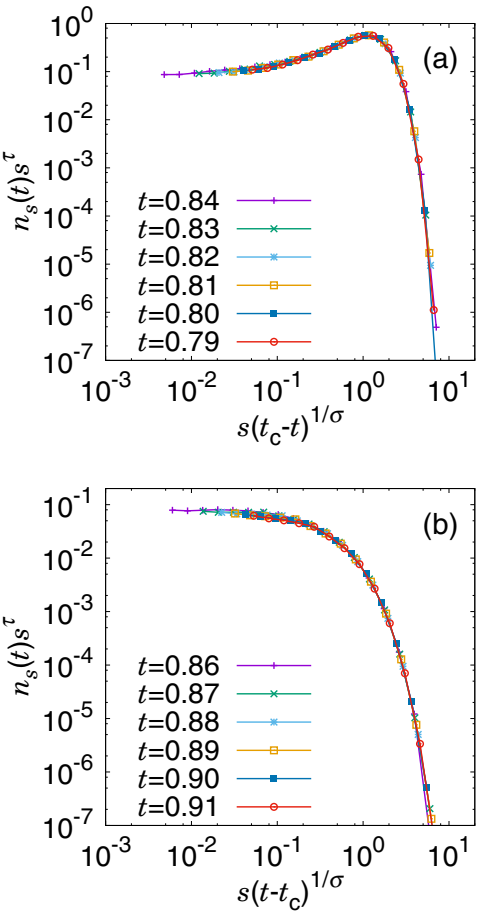

FIG. 16. The static network model with $m = 3$: Scaling plot of $n_s(t)s^{\tau}$ versus $s|t - t_c|^{1/\sigma}$ (a) for $t < t_c$ and (b) for $t > t_c$. Data points obtained from numerical simulations are well collapsed onto a single curve with $\tau = 2.105$ and $\sigma = 0.79$.

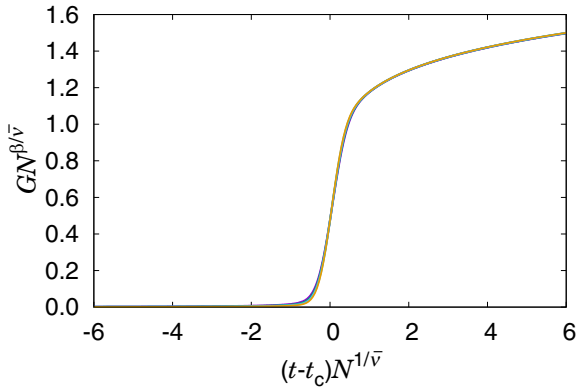

FIG. 17. The static network model with $m = 3$. Scaling plot of $GN^{\beta/\bar{\nu}}$ versus $(t - t_c)N^{1/\bar{\nu}}$ for different system sizes $N/10^4 = 2^7 - 2^{10}$. Data points obtained from numerical simulations are reasonably collapsed with $1/\bar{\nu} = 0.45$ and $\beta/\bar{\nu} = 0.06$.

we find that all data points of different system sizes are systematically collapsed onto a single curve when $1/\bar{\nu} = 0.45 \pm 0.05$ was used, shown in Fig. 17. This suggests that $\beta = 0.138 \pm 0.04$ and $\bar{\nu} = 2.25 \pm 0.25$. This estimated value of β is consistent within the error bar with the one obtained from the rate-equation approach in Sec. III c.

Next we examine the mean cluster size $\langle s \rangle$ as a function of t in a scaling form, i.e., $\langle s \rangle N^{-\gamma_p/\bar{\nu}}$ versus $(t - t_c)N^{1/\bar{\nu}}$ with $\gamma_p = 1.15 \pm 0.05$ and $1/\bar{\nu} = 0.45 \pm 0.05$ in Fig. 18. We find that the data are well collapsed. The obtained value from the data-collapse method is consistent with the one directed measured from the rate-equation approach in Sec. III c.

Finally, to test the hyperscaling relations, we use the obtained values of $\beta/\bar{\nu}$ and $1/\bar{\nu}$ to calculate $\beta = 0.138 \pm 0.04$ ($\beta^* = 0.207 \pm 0.06$ for $m = 3$) and $\bar{\nu} = 2.25 \pm 0.25$. Using those values, we obtain $d_u = 2.83 \pm 0.23$ and the correlation volume exponent $\bar{\nu}' \equiv d_u \nu = 1.42 \pm 0.12$, which is inconsistent with the one $\bar{\nu} = 2.25 \pm 0.25$ obtained by the data-collapse method. Thus, the hyperscaling relation $d_u - 2 + \eta = 2\beta^*/\nu$ does not hold. Moreover, using the mean-field value $\gamma = 1$ [27], we obtain $2\beta^* + \gamma = 1.42 \pm 0.12$. This value is consistent with $\bar{\nu}'$ but is not consistent with the measured value by the data-collapse method. Thus, the hyperscaling relation $2\beta^* + \gamma = \bar{\nu}$ does not hold for the static network model using the data obtained from Monte Carlo simulations.

D. Testing the hyperscaling relations by the data from the rate equation

We test the hyperscaling relation again with the data obtained by the rate-equation approach for the static network model. Specifically, to extract the finite-size effect from the rate equation, we introduce a cutoff of cluster size $s_k \equiv N_c$ and calculate the susceptibility [27] as

$$\chi = N \sum_{i}^{k} \left[3 \left(\frac{s_i}{N} \right)^2 \sum_{j}^{k} \frac{s_j}{N} + \left(\frac{s_i}{N} \right)^3 \right], \tag{6}$$

where i, j, and k are the indices of clusters and the summation runs following the ascending order of cluster size from $s_i = 1$ up to $s_k = N_c$. The cluster size with the index j satisfies the inequality $s_j > s_i$ for a given s_i. The statistics of the number of clusters of size s_i is obtained by the rate equation for the static network model Eq. (3).

The susceptibility exhibits a peak at a certain transition point $t_c(N_c)$. We plot the susceptibility versus cutoff size in a scaling form, $\chi N_c^{-\gamma/\bar{\nu}_r}$ versus $(t - t_c)N_c^{1/\bar{\nu}_r}$ in Fig. 19, where the subscript r of $\bar{\nu}_r$ indicates that $\bar{\nu}$ is obtained from the data obtained by the rate-equation method. With the choice of $\gamma = 1.01$ and $1/\bar{\nu}_r = 0.73$ ($\bar{\nu}_r \approx 1.370$), data points obtained by the rate-equation method are well collapsed onto a single curve. This value $\bar{\nu}_r \approx 1.370$ is consistent with $\bar{\nu}'$ within the error bar, and therefore the hyperscaling relation is satisfied. We also obtained $1/\bar{\nu}_r \approx 0.87(1)$ for $m = 4$. Together with this exponent, and $\beta \approx 0.042(1)$ in Table II, we find that the hyberscaling relation $2 \times 2\beta + \gamma = \bar{\nu}_r$ holds.

We note that $1/\bar{\nu}_r \approx 0.73$ for $m = 3$ was also obtained for the mean cluster size $\langle s \rangle$ together with $\gamma_p \approx 1.120(3)$ using the data-collapse method with the data obtained by the rate-equation method. This result suggests that the exponents $\bar{\nu}$ and $\bar{\nu}_r$ obtained from Monte Carlo simulations and the rate-equation approach, respectively, differ from each other.

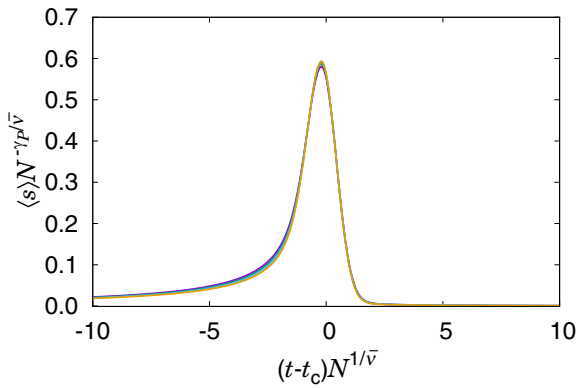

FIG. 18. The static network model with $m = 3$: Scaling plot of $\langle s \rangle N^{-\gamma_p/\bar{\nu}}$ versus $(t - t_c)N^{1/\bar{\nu}}$ for different system sizes $N/10^4 = 2^7 - 2^{10}$. Data points obtained from Monte Carlo simulations are well collapsed with $\gamma_p = 1.133$ and $1/\bar{\nu} = 0.45$.

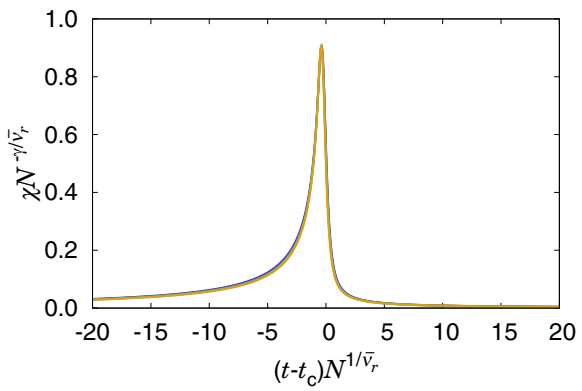

FIG. 19. The static network model with $m = 3$: Scaling plot of $\chi N_c^{-\gamma/\bar{\nu}_r}$ versus $(t - t_c)N_c^{1/\bar{\nu}_r}$ for different cutoff sizes $N_c/10^3 = 2^6 - 2^9$. Data points obtained by the rate-equation method are well collapsed with $\gamma = 1.01$ and $1/\bar{\nu}_r = 0.73$.

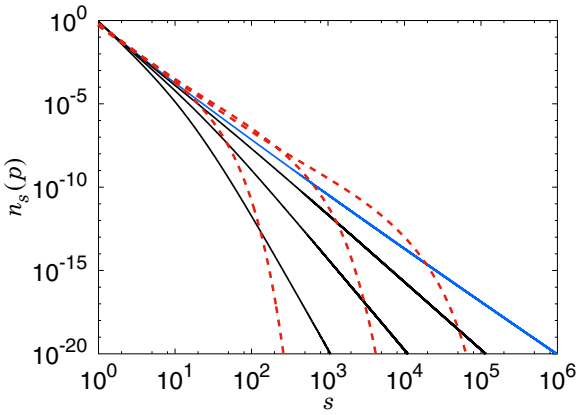

FIG. 20. The growing network model with $m = 2$: Plot of $n_s(p)$ versus s at $p = p_c$ (blue solid line), for $p > p_c$ (red dashed curves), and for $p < p_c$ (black solid lines) based on numerical values obtained from the rate equation. The transition point is estimated as $p_c = 0.125$. For $p \leqslant p_c$, $n_s(p)$ decays in a power-law manner, indicating that the transition is infinite order.

In the EP problem, due to the suppression effect, near the transition point, there exists a hump in the tail part of the cluster size distribution. The hump size reduces as the system size is increased; however, the systems of which sizes are feasible by Monte Carlo simulations still contain big humps. The correlation size exponent can be distorted by this hump in finite-size scaling analysis with Monte Carlo simulation data.

V. COMPARISON OF $n_s(p)$ FOR THE GROWING NETWORK MODEL WITH DIFFERENT m VALUES

It is interesting to note that the percolation occurring in the growing network model with $m \geqslant 3$ is a second-order transition, whereas it is of infinite order when $m = 2$. To understand the underlying mechanism between this difference, we investigate the cluster size distribution $n_s(p)$ for $m = 2$. As shown in Fig. 20, $n_s(p)$ decays in a power-law manner for $p \leqslant p_c$, while it exhibits crossover behavior for $p > p_c$. The power-law behavior of $n_s(p)$ for $p \leqslant p_c$ implies that the region $p \leqslant p_c$ is in the critical phase, which is a noticeable feature of the infinite-order transition. Intuitively, for $m = 2$, when $p \leqslant p_c$, the fraction of nodes that belong to small-size clusters is relatively small compared with the one for the model showing second-order phase transition, for instance, the case of $m \geqslant 3$ in Fig. 1. Instead, the power-law behavior sustains even to the tail region of the cluster size distribution. However, when $m \geqslant 3$, the formation of large-size clusters is suppressed by the Achlioptas rule, which leads to the crossover behavior to the exponential decay in the tail region of the cluster size distribution for $p < p_c$ for the case $m = 3$. Thus, the percolation transition in the growing network model for $m \geqslant 3$ becomes second order.

VI. SUMMARY AND DISCUSSION

We have investigated properties the percolation transition under the Achlioptas processes with general m-candidate rule on both the growing and the static ER network models using the rate-equation approaches and numerical simulations. For the growing network model, as m is increased from two to three, the type of percolation transition changes from an infinite-order one to a second-order one. The Achlioptas rule [16] yields the suppression effect against the growth of large clusters, which causes the tail part of the cluster size distribution to change from a power-law form to an exponential-decay form. Thus, the transition type changes to the second-order transition. On the other hand, in the static network model, the type of the phase transition remains the same as the second-order transition, even when m is increased.

Moreover, we showed that the critical exponent β decreases algebraically with increasing m in the growing network model; however, it decays exponentially in the static network model. This fact implies that the suppression effect in the growing network model is weaker than that in the static network model. Furthermore, we obtained other critical exponents for general m in both the growing and the static network models. We also found that the scaling relations $\beta = (2-\tau)/\sigma$ and $\gamma_p = (3-\tau)/\sigma$ hold for general m [1,2]. Importantly, the hyperscaling relations $d - 2 + \eta = 2\beta^*/\nu$ and $\bar{\nu} = 2\beta^* + \gamma$ also hold in the growing and static network models, where β^* and γ replace the conventional exponents β and γ_p of the order parameter and the mean cluster size. Here $\beta^* = (m/2)\beta$ and γ in Eq. (6), which take into account of the EP rule of multiple node candidates. We noticed that the Monte Carlo simulation method did not produce the correlation size exponent $\bar{\nu}$ correctly for the static network model.

ACKNOWLEDGMENTS

This work was supported by the National Research Foundation of Korea (NRF) through Grants No. NRF-2014R1A3A-2069005 (B.K.) and No. NRF-2014R1A1A2057396 (S.-W.S), SNU R&D program (B.K.), and the TJ Park Science Fellowship of POSCO TJ Park Foundation (S.-W.S.).

[1] D. Stauffer, Phys. Rep. **54**, 1 (1979).
[2] D. Stauffer and A. Aharony, *Introduction to Percolation Theory*, 2nd ed. (Taylor & Francis, London, 1994).
[3] P. J. Flory, J. Am. Chem. Soc. **63**, 3083 (1941).
[4] S. R. Broadbent and J. M. Hammersley, Proc. Cambr. Philos. Soc. **53**, 629 (1957).
[5] E. M. Hendriks, M. H. Ernst, and R. M. Ziff, J. Stat. Phys. **31**, 519 (1983).
[6] F. Leyvraz, Phys. Rep. **383**, 95 (2003).
[7] P. Grassberger, Math. Boisci. **63**, 157 (1983).
[8] D. Mollison, J. R. Statist. Soc. B **39**, 283 (1977).
[9] J. D. Murray, *Mathematical Biology*, 3rd ed. (Springer, Berlin, 2005).
[10] J. L. Cardy and P. Grassberger, J. Phys. A: Math. Gen. **18**, L267 (1985).
[11] M. Walther, D. G. Cooke, C. Sherstan, M. Hajar, M. R. Freeman, and F. A. Hegmann, Phys. Rev. B **76**, 125408 (2007).
[12] S. Boettcher, V. Singh, and R. M. Ziff, Nat. Commun. **3**, 787 (2012).

[13] D. S. Callaway, J. E. Hopcroft, J. M. Kleinberg, M. E. J. Newman, and S. H. Strogatz, Phys. Rev. E **64**, 041902 (2001).
[14] J. Kim, P. L. Krapivsky, B. Kahng, and S. Redner, Phys. Rev. E **66**, 055101(R) (2002).
[15] J. Chalupa, P. L. Leath, and G. R. Reich, J. Phys. C **12**, L31 (1979).
[16] D. Achlioptas, R. M. D'Souza, and J. Spencer, Science **323**, 1453 (2009).
[17] S. V. Buldyrev, R. Parshani, G. Paul, H. E. Stanley, and S. Havlin, Nature **464**, 1025 (2010).
[18] S.-W. Son, P. Grassberger, and M. Paczuski, Phys. Rev. Lett. **107**, 195702 (2011).
[19] R. A. da Costa, S. N. Dorogovtsev, A. V. Goltsev, and J. F. F. Mendes, Phys. Rev. Lett. **105**, 255701 (2010).
[20] O. Riordan and L. Warnke, Science **333**, 322 (2011).
[21] Y. S. Cho, S. Hwang, H. J. Herrmann, and B. Kahng, Science **339**, 1185 (2013).
[22] P. Grassberger, C. Christensen, G. Bizhani, S.-W. Son, and M. Paczuski, Phys. Rev. Lett. **106**, 225701 (2011).
[23] R. K. Pan, M. Kivelä, J. Saramäki, K. Kaski, and J. Kertész, Phys. Rev. E **83**, 046112 (2011).
[24] S. D. Yi, W. S. Jo, B. J. Kim, and S.-W. Son, Europhys. Lett. **103**, 26004 (2013).
[25] W. S. Jo, S. D. Yi, B. J. Kim, and S.-W. Son, J. Kor. Phys. Soc. **65**, 1985 (2014).
[26] R. A. da Costa, S. N. Dorogovtsev, A. V. Goltsev, and J. F. F. Mendes, Phys. Rev. E **89**, 042148 (2014).
[27] R. A. da Costa, S. N. Dorogovtsev, A. V. Goltsev, and J. F. F. Mendes, Phys. Rev. E **90**, 022145 (2014).
[28] P. Erdős and A. Rényi, Publ. Math. Inst. Hungar. Acad. Sci. **5**, 17 (1960).